Histol Histopathol (2022) 37: 985-997

http://www.hh.um.es

Histology and Histopathology
From Cell Biology to Tissue Engineering

ORIGINAL ARTICLE **Open Access**

Knockdown of circRNA circEBF1 inhibits cutaneous squamous cell carcinoma progression by regulating the miR-1247-5p/CSF3 axis

Dong Yin[1], Guo Wei[2], Xiaoyan Sun[1] and Yan Yin[3]

[1]Department of Dermatology, Shaanxi Provincial People's Hospital, Xi'an City, Shaanxi Province, [2]Department of Dermatology, The Second Hospital of Shandong University, Jinan City, Shandong Province and [3]Department of Gastroenterology, First Affiliated Hospital of Xi'an Jiaotong University, Xi'an City, Shaanxi Province, China

Summary. Background. Cutaneous squamous cell carcinoma (CSCC) is one of the causes of cancer-related death worldwide. Circular RNAs (circRNAs) play a vital role in the pathological process of many malignant tumors. This study aimed to explore the specific role and potential mechanism of circRNA EBF transcription factor 1 (circEBF1) in CSCC.

Methods. The levels of circEBF1, microRNA-1247-5p (miR-1247-5p) and colony stimulating factor 3 (CSF3) were determined by quantitative real-time PCR and Western blot. Cell proliferation was assessed by colony formation assay. Cell migration, invasion and apoptosis were evaluated by Transwell, wound healing, flow cytometry and Western blot assays. Cellular glycolysis, including glucose consumption, lactate production, and ATP level, was detected by commercial kits. The binding relationship between miR-1247-5p and circEBF1 or CSF3 was verified by dual-luciferase reporter assay, RNA immunoprecipitation (RIP) assay and RNA pull-down assay. Xenograft experiment was conducted to analyze tumor growth *in vivo*.

Results. circEBF1 and CSF3 were up-regulated, while miR-1247-5p was down-regulated in CSCC tissues and cells. Interference of circEBF1 hindered the proliferation, migration, invasion, and glycolysis of CSCC cells and promoted apoptosis. In addition, circEBF1 sponged miR-1247-5p to regulate CSCC cell development. Also, miR-1247-5p suppressed CSCC cell progression by inhibiting CSF3. Moreover, depletion of circEBF1 blocked CSCC tumor growth *in vivo*.

Conclusion. Down-regulation of circEBF1 impeded CSCC progression by regulating the miR-1247-5p/CSF3 pathway, suggesting that circEBF1 might be a promising therapeutic target for CSCC.

Key words: Cutaneous squamous cell carcinoma, circEBF1, miR-1247-5p, CSF3

Corresponding Author: Dong Yin, MM, Department of Dermatology, Shanxi Provincial People's Hospital, No.256 Youyi West Road, Beilin District, Xi'an City, Shaanxi Province, 710068, PR China. e-mail: dryindong@126.com

DOI: 10.14670/HH-18-468

Introduction

Cutaneous squamous cell carcinoma (CSCC) is the second most frequent nonmelanoma skin cancer (Navarrete-Dechent et al., 2015). CSCC originates from keratinocytes and accounts for about 20% of keratinocyte carcinomas (Nagarajan et al., 2019). In addition, metastasis occurs in 3-7% of CSCC patients, and the mortality rate of metastatic CSCC is as high as 70% (Ratushny et al., 2012; Karia et al., 2013). Although surgery combined with chemotherapy and radiotherapy is effective, the treatment of metastatic CSCC still faces great challenges (Que et al., 2018). Therefore, elucidating the underlying pathogenesis of CSCC is essential for identifying new biomarkers to develop more effective treatment strategies.

Circular RNAs (circRNAs) are single-stranded RNA molecules and are formed by back-splicing without 5' to 3' polarity (Zhang et al., 2018). CircRNAs have been identified as tissue-specific and disease-specific and are promising therapeutic targets for human diseases (Braicu et al., 2019). CircRNAs have been demonstrated to exert indispensable effects in tumor occurrence and development (Li et al., 2020). For example, hsa_circ_0002577 was conspicuously overexpressed in endometrial cancer, and its down-regulation restrained the growth and metastasis of endometrial carcinoma cells by mediating the PI3K/Akt pathway (Wang et al., 2020). Chen et al. revealed that interference of circ_0008532 suppressed cell invasion in bladder cancer through the competitive endogenous RNA (ceRNA) mechanism (Chen et al., 2020a). CircEBF1 (hsa_circ_0074817) derived from the EBF transcription

©The Author(s) 2022. **Open Access.** This article is licensed under a Creative Commons CC-BY International License.

factor 1 (EBF1) gene was strikingly up-regulated in CSCC (Sand et al., 2016). However, the role and underlying mechanism of circEBF1 in CSCC are still unknown.

In terms of mechanism, circRNAs can mediate gene expression by sponging microRNAs (miRNAs) to indirectly regulate the downstream target genes of miRNAs (Harper et al., 2019). Additionally, plentiful studies have verified that miRNA dysregulation is strongly related to CSCC progression (Yu and Li, 2016; Konicke et al., 2018; Garcia-Sancha et al., 2019). Ectopic expression of miR-664 facilitated the malignant phenotype of CSCC by inhibiting IRF2 (Li et al., 2019). Besides, An et al. discovered that miR-1247-5p was markedly diminished and directly bound to circ_0070934 in CSCC (An et al., 2019). Nevertheless, the exact mechanism of miR-1247-5p in CSCC has not been fully elucidated.

In our research, the expression pattern of circEBF1 was first investigated. Furthermore, a battery of functional experiments were conducted to verify whether circEBF1 acted as a ceRNA to regulate colony stimulating factor 3 (CSF3) expression by absorbing miR-1247-5p.

Materials and methods

Specimen collection and cell culture

CSCC specimens (n=43) and adjacent non-tumor tissues (n=43) were collected from CSCC patients diagnosed at Shaanxi Provincial People's Hospital. Each patient in this study signed the written informed consent. None of the patients received any preoperative treatment. This research was authorized by the Ethics Committee of Shanxi Provincial People's Hospital. Human keratinocyte cell line HaCaT was commercially acquired from China Center for Type Culture Collection (Wuhan, China). CSCC cell lines (SCC13 and HSC5) were purchased from Ningbo Mingzhou Biological Technology Co., Ltd. (Ningbo, China). All cells were cultured in DMEM (Invitrogen, Carlsbad, CA, USA) containing 10% FBS (Invitrogen) at 37°C with 5% CO_2.

Cell transfection

circEBF1 siRNA (si-circEBF1), miR-1247-5p mimics (miR-1247-5p), miR-1247-5p inhibitor (in-miR-1247-5p), CSF3 overexpression vector (CSF3), and the matched controls (si-NC, miR-NC, in-miR-NC, and pcDNA) were synthesized from HanBio (Shanghai, China). When cell confluence reached 70%, cell transfection was carried out using Lipofectamine 3000 (Invitrogen).

Quantitative real-time PCR (qRT-PCR)

TRIzol reagent (Invitrogen) was used to extract RNA. Next, complementary DNA was synthesized via the specific reverse transcription kit (Vazyme, Nanjing, China). Afterwards, qRT-PCR was implemented via SYBR Green Master Mix (Vazyme). The primers included: circEBF1-F: 5'- ATCCCTGGTGTTGTGGA AGT-3', circEBF1-R, 5'-TGATGATCACAGTCG CACCT-3'; EBF1-F: 5'-ATGTCTCCGAGGCATC ACAAGC-3', EBF1-R, 5'-TCATGCTCGTGGTGA CGGAGTT-3'; miR-1247-5p-F: 5'-GGGACCCGTCC CGTTCGTC-3', miR-1247-5p-R, 5'- CAGTGCGTGT CGTGGAGT-3'; CSF3-F: 5'-TCCAGGAGAAGCTGG TGAGTGA-3', CSF3-R, 5'-CGCTATGGAGTTGGCT CAAGCA-3'; GAPDH-F: 5'-TCACCAGGGCTGCTT TTAAC-3', GAPDH-R: 5'-GACAAGCTTCCCGTT CTCAG-3'; U6-F: 5'-CTCGCTTCGGCAGCACATA-3', U6-R: 5'-AACGCTTCACGAATTTGCGT-3'. The RNA levels were analyzed via the $2^{-\Delta\Delta Ct}$ method. GAPDH (for circEBF1, EBF1 and CSF3) or U6 (for miR-1247-5p) was used as an internal control.

CircRNA identification

RNase R treatment was used for degrading linear RNAs. RNA (2 μg) was incubated with RNase R (3U/μg) (Seebio, Shanghai, China) for 30 min. Next, circEBF1 and EBF1 levels were assessed by qRT-PCR.

For Actinomycin D assay, cells (2×10^4 cells/well) were seeded into a 24-well plate and exposed to 2 μg/mL Actinomycin D (Sigma-Aldrich, St. Louis, MO, USA) for 0, 4, 8 and 12 h to block transcription. Thereafter, qRT-PCR was used for measuring circEBF1 and EBF1 expression.

Colony formation assay

After digestion with 0.25% trypsin (Solarbio, Beijing, China), SCC13 and HSC5 cells (200 cells/well) were seeded into 6-well plates. Following 14 days of culture, SCC13 and HSC5 cells were fixed with paraformaldehyde (4%), followed by staining with crystal violet (0.5%, Solarbio).

5-Ethynyl-2'-deoxyuridine (EdU) assay

EdU kit (Guangzhou, China) was used to test DNA synthesis. In short, cells (2×10^4 cells/well) were seeded into a 24-well plate. After treatment, cells were incubated with EdU solution (50 μM). After incubation for 2 h, these cells were fixed with paraformaldehyde (4%) and treated with Triton-X-100 (0.5%), followed by staining with Apollo reaction in a dark place for 0.5 h. After staining with DAPI, these cells were observed with a fluorescence microscope (Leica, Wetzlar, Germany) at 200× magnification.

Transwell assay

Transwell chambers (Corning Life Sciences,

Corning, NY, USA) with or without Matrigel (Corning Life Sciences) were applied to evaluate the invasive and migratory capacities of SCC13 and HSC5 cells. Briefly, the cells (2×10^4 cells/well) were seeded into the top chamber, and DMEM containing 10% FBS was seeded into the bottom chamber. Twenty-four hours later, the cells on the lower surface were stained with crystal violet (0.5%, Solarbio) and counted with a microscope (100×, Leica).

Wound healing assay

After transfection, SCC13 and HSC5 cells (1×10^4 cells/well) were injected into a 12-well plate. Subsequently, a linear wound was created using a sterile pipette tip. After 24 h of incubation, these cells were photographed with a microscope (Leica). ImageJ software was used to measure the percentage of wound closure.

Flow cytometry

After collecting transfected cells (1×10^6 cells), these cells were washed with PBS (Seebio). After resuspending in binding buffer, the cells were stained with Annexin V-FITC and PI (Vazyme), followed by the detection of apoptotic cells using a flow cytometer (Beckman Coulter, Miami, FL, USA).

Western blot assay

RIPA lysis buffer (Beyotime, Shanghai, China) was used for the extraction of protein. After measuring protein concentration, protein samples were subjected to 10% SDS-PAGE, then transferred onto PVDF membranes (Millipore, Billerica, MA, USA). Following blockage using 5% skim milk (Beyotime), the membranes were incubated with the primary antibodies against Bcl-2 (1:1000, ab194583, Abcam, Cambridge, UK), Bax (1:500, ab53154, Abcam), N-cadherin (1:2000, ab18203, Abcam), E-cadherin (1:20000, ab40772, Abcam), CSF3 (1:1000, ab9691, Abcam) and β-actin (1:2000, ab8227, Abcam) for 12-16 h at 4°C. Subsequently, these membranes were probed with an HRP-conjugated secondary antibody (1:5000, ab205718, Abcam). Finally, the visualization of protein blots was achieved using an ECL luminescence reagent (Absin, Shanghai, China).

Glycolysis detection

Glucose Assay Kit and Lactate Assay Kit (BioVision, Milpitas, CA, USA) were applied for examining glucose consumption and lactate production. ATP production was measured by ATP Detection Assay Kit (Abcam).

Dual-luciferase reporter assay

The fragments of circEBF1 or 3'UTR region of CSF3 containing the wild-type or mutant miR-1247-5p-binding sites were synthesized and cloned into the pmirGLO vector (LMAI Bio, Shanghai, China), generating circEBF1 WT/MUT or CSF3 3'UTR WT/MUT. After that, the above vectors were transfected into SCC13 and HSC5 cells (2×10^4 cells/well) together with miR-1247-5p/miR-NC. The luciferase activity was determined via Dual Luciferase Reporter Assay Kit (Vazyme).

RNA immunoprecipitation (RIP) assay

EZ-Magna RIP kit (Millipore) was utilized to conduct RIP assay. In short, cells (2×10^4 cells/well) were seeded into 24-well plates and lysed with RIP lysis buffer, followed by incubation with magnetic beads coupled with the antibody against immunoglobulin G (anti-IgG) or Argonaute2 (anti-Ago2). Thereafter, immunoprecipitated RNA was extracted after incubation with Proteinase K. Lastly, circEBF1 and miR-1247-5p enrichment were examined via qRT-PCR.

RNA pull-down assay

Biotinylated negative control (Bio-NC) and biotinylated circEBF1 WT/MUT (Bio- circEBF1 WT/MUT) were purchased from (RiboBio) and incubated with SCC13 and HSC5 cell lysates. The streptavidin magnetic beads (Invitrogen) were added into the above complex. After incubation for 0.5 h, the mixture was washed and the RNA complexes were extracted. Finally, miR-1247-5p enrichment was tested by qRT-PCR.

Xenograft assay

The animal experiment was authorized by the Animal Ethics Committee of Shanxi Provincial People's Hospital. BALB/c nude mice (n=10) were commercially obtained from Beijing Vital River (Beijing, China). Lentivirus containing circEBF1 shRNA (sh-circEBF1) or the control (sh-NC) bought from HanBio was introduced into HSC5 cells. Subsequently, the HSC5 cells (1×10^6) were subcutaneously injected into the right armpits of the mice. Tumor volume was examined every 7 days. Following 28 days, these mice were sacrificed, and excised tissues were removed and harvested. The expression levels of circEBF1, miR-1247-5p and CSF3 in the excised tumors were tested using qRT-PCR, Western blot, or immunohistochemistry (IHC) analysis.

IHC analysis

After fixing in 10% formalin (Beyotime), the tissues were embedded in paraffin and cut. After that, consecutive thick sections (5 μm) were incubated with the primary antibody against CSF3 (1:500, ab270267, Abcam). After incubation with secondary antibody (1:5000, ab205718, Abcam) for 1 h, the slides were

stained with 3,3'-Diaminobenzidine (DAB) solution (Sangon, Shanghai, China) and counterstained using hematoxylin (Beyotime). All images were acquired using a microscope (Leica).

Statistical analysis

Data are displayed as mean ± standard deviation using GraphPad Prism 7 software (GraphPad, San Diego, CA, USA). The differences were determined by Student's t-test and one-way analysis of variance. When P-value<0.05, the difference was considered statistically significant. All experiments were independently repeated three times.

Results

circEBF1 was up-regulated in CSCC tissues and cells

Firstly, the expression pattern of circEBF1 in CSCC tissues and adjacent normal tissues was determined using qRT-PCR. The results suggested that circEBF1 level in CSCC tissues was significantly higher than that in normal tissues (Fig. 1A). Meanwhile, circEBF1 expression was strikingly increased in CSCC cells (SCC13 and HSC5) compared with human keratinocytes (HaCaT) (Fig. 1B). In addition, RNase R digestion assay was applied to analyze the circular characteristic of circEBF1. The results showed that circEBF1 was resistant to RNase R compared with linear EBF1, indicating that circEBF1 was a stable circular RNA (Fig. 1C,D). Actinomycin D assay exhibited that the half-life of circEBF1 transcript exceeded 12 h, while the half-life of EBF1 was about 8 h (Fig. 1E,F), suggesting that circEBF1 transcript was more stable than EBF1 transcript.

Silencing of circEBF1 inhibited the proliferation, migration, invasion, and glycolysis of CSCC cells and induced apoptosis

To investigate the function of circEBF1 in CSCC progression, loss-of-function experiments were carried out in SCC13 and HSC5 cells after transfection with circEBF1 siRNA. As displayed in Fig. 2A, the knockdown efficiency of si-circEBF1 was significant. Colony formation assay and EdU assay showed that down-regulation of circEBF1 hindered colony formation

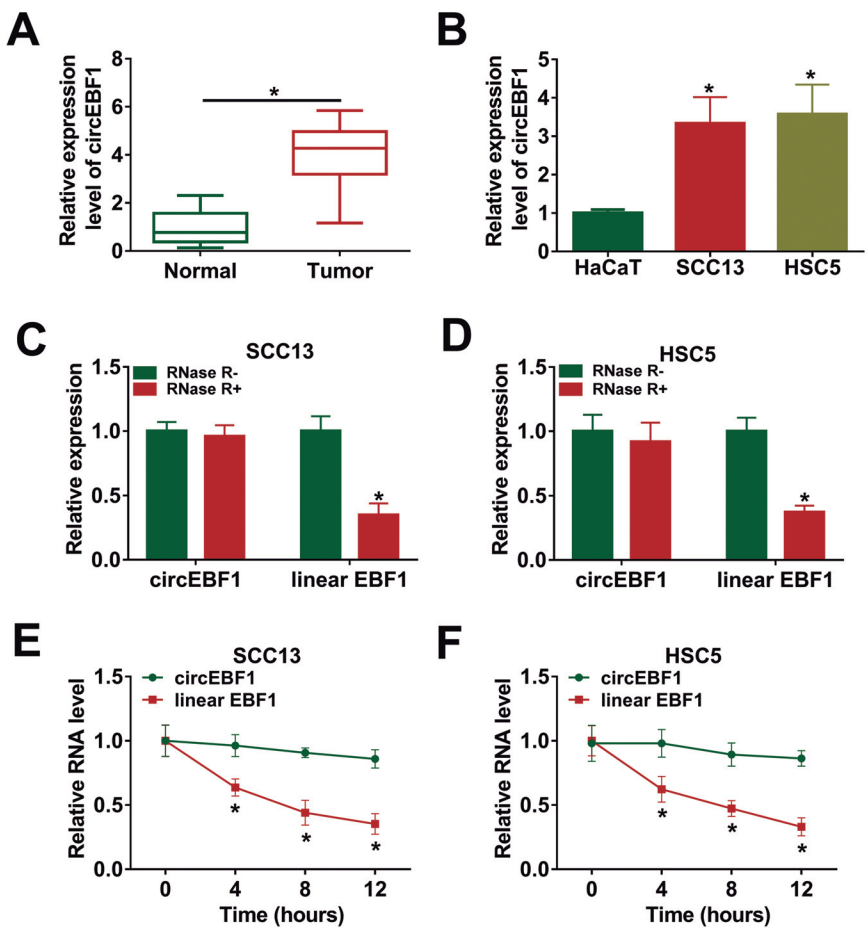

Fig. 1. Expression of circEBF1 in CSCC tissues and cells. **A.** The expression level of circEBF1 was detected using qRT-PCR in CSCC tissues (n=43) and adjacent normal tissues (n=43). **B.** The level of circEBF1 in CSCC cells (SCC13 and HSC5) and human keratinocyte cell line (HaCaT) was examined using qRT-PCR. **C-F.** After treatment with RNase R and Actinomycin D, qRT-PCR was used to measure the levels of circEBF1 and linear EBF1. *P<0.05.

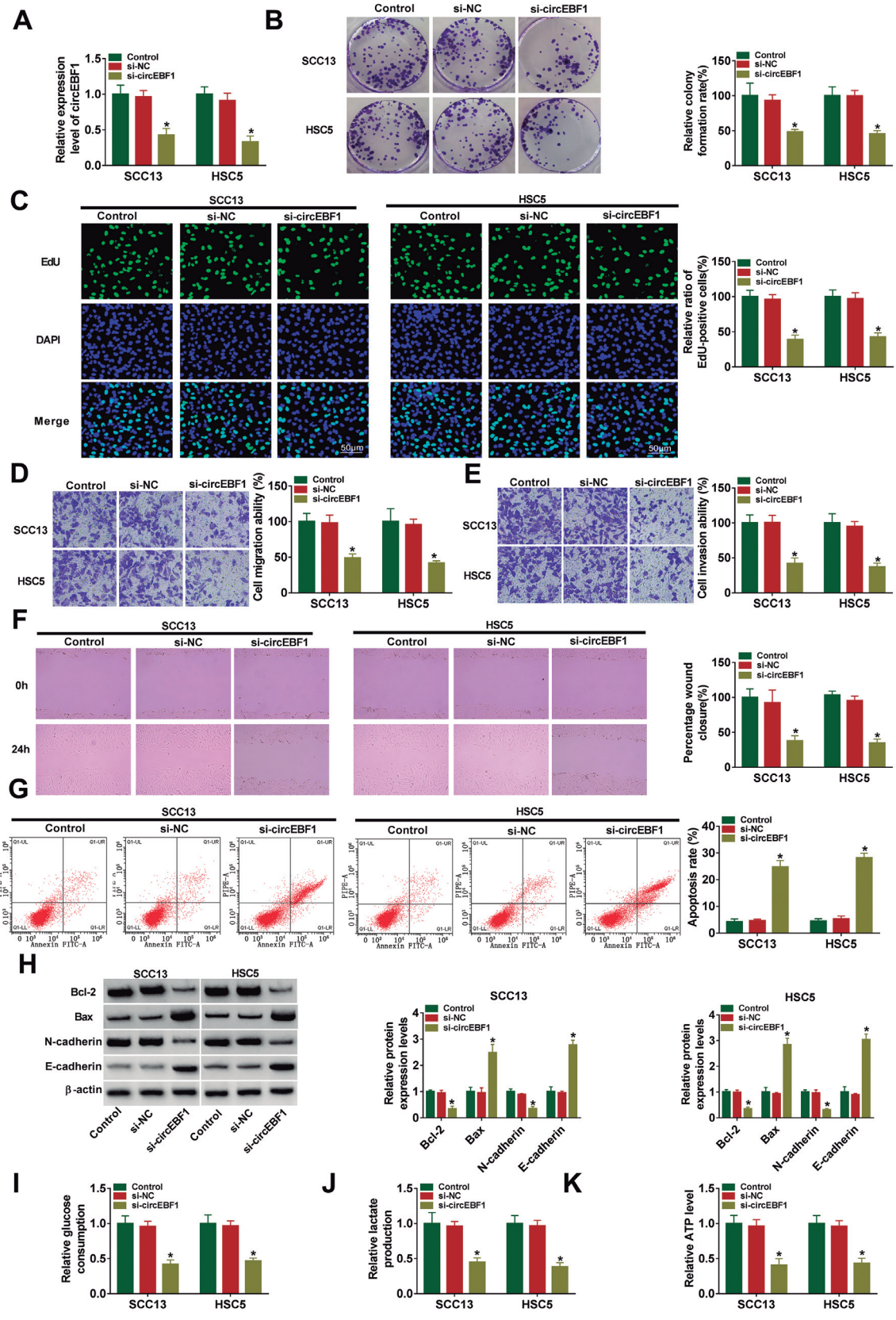

Fig. 2. Silencing of circEBF1 inhibited the proliferation, migration and invasion of CSCC cells and induced apoptosis. SCC13 and HSC5 cells were introduced with si-NC or si-circEBF1, respectively. **A.** The expression of circEBF1 was measured using qRT-PCR. **B.** Cell colony formation ability was assessed by colony formation assay. **C.** DNA synthesis was determined by EdU assay. **D, E.** Cell migration and invasion were determined by Transwell assay. **F.** Cell migration was evaluated by wound healing assay. **G.** Cell apoptosis was detected by flow cytometry. **H.** The levels of apoptosis-related proteins (Bcl-2 and Bax) and invasion-related proteins (N-cadherin and E-cadherin) were detected by Western blot assay. **I-K.** Glucose consumption, lactate production, and cellular ATP level were assessed by corresponding kits. *P<0.05. D, E, x 100; F, x 40.

ability and reduced EdU-positive cells relative to the control group (Fig. 2B,C), indicating that circEBF1 depletion inhibited cell proliferation. Transwell analysis revealed that circEBF1 silencing restrained the migratory and invasive capacities of CSCC cells compared with the control group (Fig. 2D,E). Consistently, wound healing assay showed that knockdown of circEBF1 suppressed CSCC cell migration compared to the control group (Fig. 2F). Flow cytometry exhibited that introduction of si-circEBF1 remarkably increased the apoptosis rate of SCC13 and HSC5 cells compared with the si-NC group (Fig. 2G). In

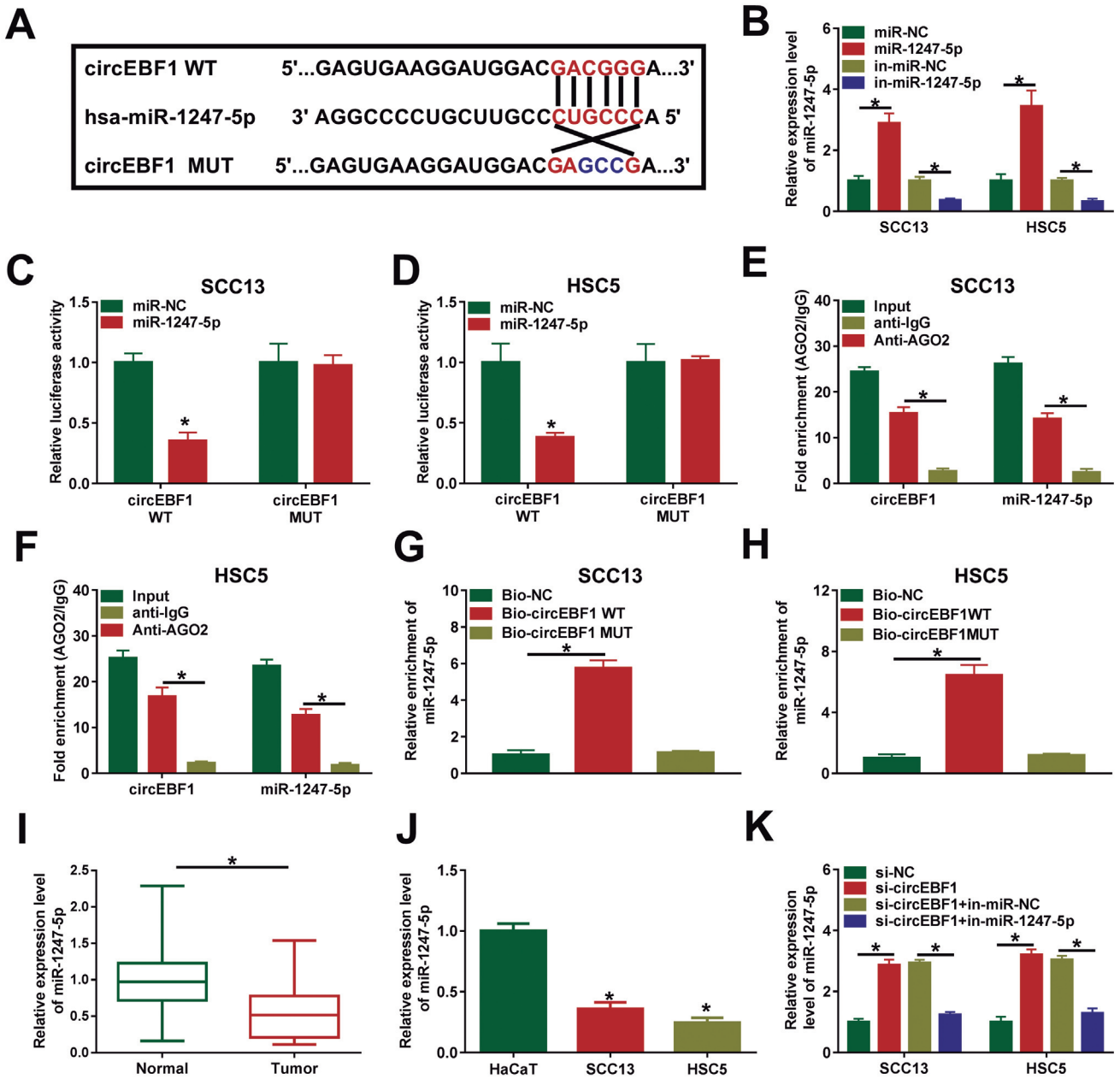

Fig. 3. circEBF1 acted as a sponge for miR-1247-5p. **A.** The putative binding site between circEBF1 and miR-1247-5p was predicted by the Circular RNA Interactome. **B.** The expression of miR-1247-5p was examined using qRT-PCR in SCC13 and HSC5 cells transfected with miR-NC or miR-1247-5p. **C, D.** The luciferase activity was tested in SCC13 and HSC5 cells by dual-luciferase reporter assay. **E, F.** The enrichment of circEBF1 and miR-1247-5p in SCC13 and HSC5 cells was examined by RIP assay. **G, H.** The enrichment of SCC13 and HSC5 was examined by RNA pull-down assay in SCC13 and HSC5 cells incubated with Bio-NC, Bio-circEBF1 WT, or Bio- circEBF1 MUT. **I, J.** The level of miR-1247-5p in CSCC tissues (n=43) and cells (SCC13 and HSC5) was determined by qRT-PCR. **K.** After transfection with si-NC, si-circEBF1, si-circEBF1+in-miR-NC, or si-circEBF1+ in-miR-1247-5p, miR-1247-5p level was measured by qRT-PCR. *P<0.05.

addition, Western blot analysis showed that si-circEBF1 transfection resulted in significant decreases in Bcl-2 (anti-apoptotic molecule) and N-cadherin (a mesenchymal marker) levels and marked increases in Bax (pro-apoptotic molecule) and E-cadherin (an epithelial marker) levels (Fig. 2H). Most of the fast-growing malignant cells have active glycolysis and gain more energy through glycolysis. Next, we explored the impact of circEBF1 on glycolysis. Interference of circEBF1 inhibited glycolysis by decreasing glucose consumption, lactate production, and ATP level in SCC13 and HSC5 cells (Fig. 2I-K). These results indicated that depletion of circEBF1 impeded the proliferation, migration, invasion, and glycolysis of

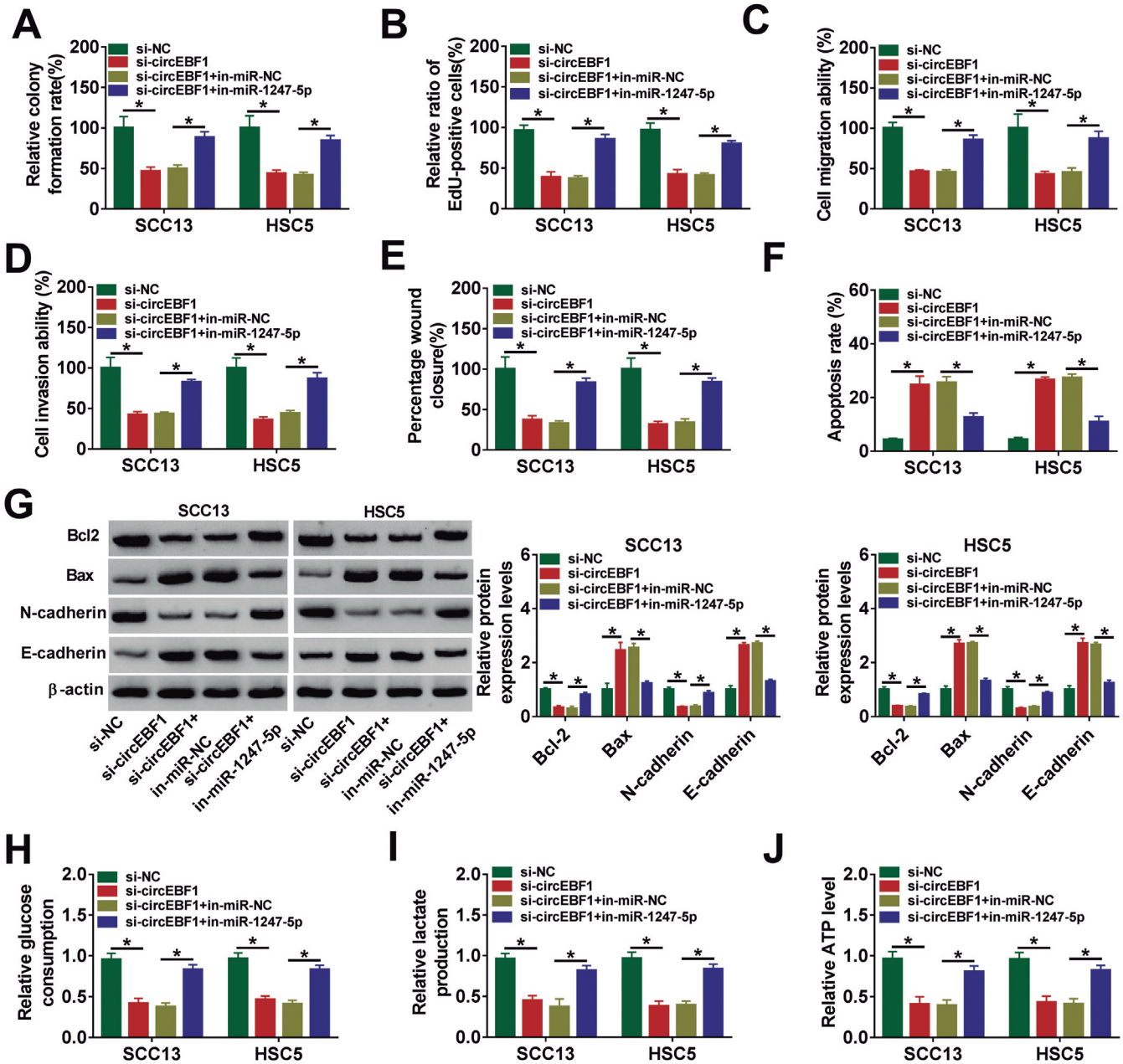

Fig. 4. Knockdown of miR-1247-5p reversed the effect of circEBF1 depletion on CSCC cell progression. SCC13 and HSC5 cells were transfected with si-NC, si-circEBF1, si-circEBF1+in-miR-NC or si-circEBF1+in-miR-1247-5p, respectively. After transfection, colony formation, EdU, Transwell, wound healing, flow cytometry and Western blot assays were used to detect colony formation rate **(A)**, DNA synthesis **(B)**, cell migration and invasion **(C-E)**, cell apoptosis rate **(F)** and relative protein levels **(G)**. **H-J.** Glucose consumption, lactate production, and ATP level were determined by corresponding commercial kits *P<0.05.

CSCC cells and triggered apoptosis.

CircEBF1 acted as a sponge for miR-1247-5p

Bioinformatics analysis (Circular RNA Interactome; https://circinteractome.irp.nia.nih.gov/) predicted the potential targets of circEBF1, and the results showed that miR-1247-5p might be a potential target miRNA of circEBF1 (Fig. 3A). Subsequently, qRT-PCR analysis confirmed that the overexpression efficiency of miR-1247-5p mimics was significant (Fig. 3B). To verify the binding relationship between circEBF1 and miR-1247-5p, dual-luciferase reporter assay, RIP assay, and RNA pull-down assay were carried out in SCC13 and HSC5 cells. As shown in Fig. 3C,D, miR-1247-5p mimics remarkably reduced the luciferase activity of circEBF1 WT, but did not affect circEBF1 MUT. RIP assay revealed that the enrichment of circEBF1and miR-1247-5p was markedly increased in the anti-Ago2 group compared to the anti-IgG group (Fig. 3E,F). RNA pull-down assay exhibited that Bio-circEBF1 WT led to higher miR-1247-5p enrichment than Bio-circEBF1 MUT or Bio-NC in SCC13 and HSC5 cells (Fig. 3G,H). Besides, the expression pattern of miR-1247-5p in CSCC tissues and cells was analyzed using qRT-PCR. The results suggested that miR-1247-5p level in CSCC tissues and cells was strikingly decreased compared with normal tissues and HaCaT cells (Fig. 3I,J). Furthermore,

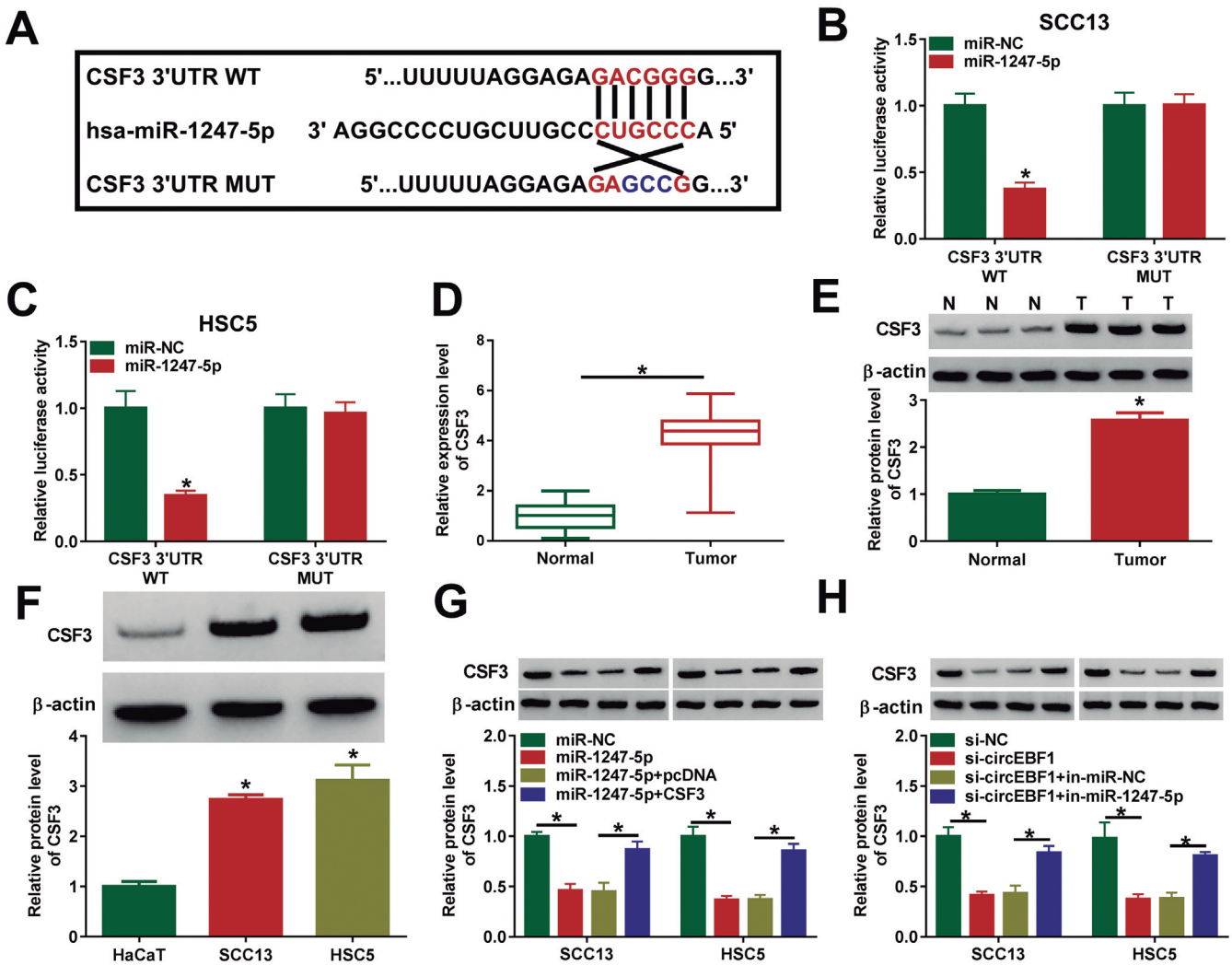

Fig. 5. miR-1247-5p directly targeted CSF3. **A.** The predicted binding site between miR-1247-5p and CSF3 was predicted by TargetScan. **B, C.** The luciferase activity was detected in SCC13 and HSC5 cells co-transfected with CSF3 3'UTR WT or CSF3 3'UTR MUT and miR-NC or miR-1247-5p. **D, E.** The mRNA and protein levels of CSF3 in CSCC tissues (n=43) and adjacent normal tissues (n=43) were examined by qRT-PCR and Western blot. **F.** CSF3 protein expression in SCC13, HSC5 and HaCaT cells was detected by Western blot. **G.** CSF3 protein level was measured by Western blot in SCC13 and HSC5 cells transfected with miR-NC, miR-1247-5p, miR-1247-5p+pcDNA, or miR-1247-5p+CSF3. **H.** CSF3 protein level was determined by Western blot in SCC13 and HSC5 cells transfected with si-NC, si-circEBF1, si-circEBF1+in-miR-NC or si-circEBF1+in-miR-1247-5p. *P<0.05.

si-circEBF1 transfection significantly elevated the expression of miR-1247-5p compared with the si-NC group, and the introduction of in-miR-1247-5p abolished the increased expression of miR-1247-5p caused by circEBF1 interference (Fig. 3K). These data evidenced that circEBF1 negatively regulated miR-1247-5p.

Knockdown of miR-1247-5p reversed the effect of circEBF1 depletion on CSCC cell progression

To explore whether circEBF1 regulates CSCC development by sponging miR-1247-5p, rescue experiments were performed in SCC13 and HSC5 cells. Knockdown of circEBF1 suppressed the proliferative capability of SCC13 and HSC5 cells, while this impact was partially eliminated by down-regulating miR-1247-5p (Fig. 4A,B). Moreover, circEBF1 depletion inhibited cell migration and invasion and accelerated apoptosis in SCC13 and HSC5 cells, whereas co-transfection of si-circEBF1 and in-miR-1247-5p reversed these effects (Fig. 4C-F). Simultaneously, knockdown of miR-1247-5p overturned the inhibition of Bcl-2 and N-cadherin expression and the promotion of Bax and E-cadherin expression caused by circEBF1 silencing (Fig. 4G). Moreover, the suppressive effects of circEBF1 down-regulation on glucose consumption, lactate production, and ATP level were abated by the inhibition of miR-1247-5p (Fig. 4H-J). These results identified that circEBF1 expedited CSCC cell progression by sponging miR-1247-5p.

miR-1247-5p directly targeted CSF3

TargetScan (http://www.targetscan.org/vert_72/) online database predicted that miR-1247-5p and CSF3 3'UTR possessed a putative binding site (Fig. 5A). Subsequently, dual-luciferase reporter assay was applied to validate the targeting relationship between miR-1247-5p and CSF3. The results showed that SCC13 and HSC5 cells co-transfected with miR-1247-5p mimics and CSF3 3'UTR WT exhibited significantly reduced luciferase activity compared to the control group (Fig. 5B,C). Additionally, qRT-PCR and Western blot assays revealed that CSF3 mRNA and protein levels were prominently increased in CSCC tissues relative to normal tissues (Fig. 5D,E). Also, the protein expression of CSF3 was remarkably elevated in SCC13 and HSC5 cells compared with HaCaT cells (Fig. 5F). As depicted in Fig. 5G, up-regulation of miR-1247-5p inhibited the protein expression of CSF3, and transfection of CSF3 overexpression vector restored the decrease in CSF3 protein level caused by up-regulation of miR-1247-5p. Furthermore, knockdown of circEBF1 markedly suppressed CSF3 protein expression in SCC13 and HSC5 cells, while the change was restored after transfection with in-miR-1247-5p (Fig. 5H). Overall, these data indicated that circEBF1 increased CSF3 expression by sponging miR-1247-5p.

CSF3 restored the inhibitory effect of miR-1247-5p on CSCC cell progression

To clarify the role of the miR-1247-5p/CSF3 axis in CSCC, SCC13 and HSC5 cells were transduced with miR-NC, miR-1247-5p, miR-1247-5p+pcDNA or miR-1247-5p+CSF3, and a series of functional experiments were performed. MiR-1247-5p overexpression restrained the proliferation, migration and invasion of SCC13 and HSC5 cells and induced cell apoptosis, while these effects were reversed by increasing CSF3 expression (Fig. 6A-F). Consistently, transfection of miR-1247-5p+CSF3 abolished the decrease in Bcl-2 and N-cadherin levels and the increase in Bax and E-cadherin levels caused by miR-1247-5p overexpression alone (Fig. 6G). Moreover, restoration of miR-1247-5p inhibited glycolysis in SCC13 and HSC5 cells, which could be reversed by elevating CSF3 expression (Fig. 6H-J). These data demonstrated that miR-1247-5p hindered CSCC cell progression by targeting CSF3.

Silencing of circEBF1 hindered CSCC growth in vivo

To investigate the effect of circEBF1 on CSCC tumorigenesis *in vivo*, HSC5 cells transfected with sh-NC or sh-circEBF1 were subcutaneously injected into nude mice. First of all, the qRT-PCR analysis showed that sh-circEBF1 transfection significantly down-regulated the expression of circEBF1 compared with the control group (Fig. 7A). In addition, tumor volume and weight were remarkably reduced in the sh-circEBF1 group compared to the sh-NC group (Fig. 7B,C). Furthermore, qRT-PCR and Western blot assays revealed that the introduction of sh-circEBF1 prominently increased miR-1247-5p level and decreased CSF3 mRNA and protein levels compared with the control group (Fig. 7D-F). IHC analysis showed that circEBF1 down-regulation suppressed CSF3 expression in tumor tissues (Fig. 7G). These data evidenced that circEBF1 depletion blocked tumor growth *in vivo*.

Discussion

CSCC is a common malignancy among Caucasians, and its incidence is rising (Yesantharao et al., 2017). Ultraviolet radiation (UVR), the main risk factor for CSCC, leads to excessive proliferation of epidermal keratinocytes by inducing extensive accumulation of DNA damage (Inman et al., 2018). Recently, non-coding RNAs have been discovered as new biomarkers or therapeutic targets for diverse cancers, and circRNA has become a new research hotspot (Slack and Chinnaiyan, 2019; Li et al., 2020). In addition, high-throughput sequencing results showed that plenty of circRNAs were aberrantly expressed in CSCC, and circRNAs could participate in CSCC progression through a series of biological processes (Sand et al., 2016; Chen et al., 2020b). For example, circRNA_001937 contributed to CSCC development by competitively combining with

miRNA-597-3p to activate FOSL2 (Gao et al., 2020). Hsa_circ_0070934 accelerated the growth and invasion of CSCC cells by decoying miR-1236-3p and up-regulating HOXB7 (Zhang et al., 2020). However, the research on the role of circRNA in CSCC is limited. Hence, the purpose of our research was to clarify the exact role and possible mechanism of circEBF1 in CSCC.

In this research, we identified that circEBF1 was prominently increased in CSCC, and its down-regulation hindered the development of CSCC. Besides, emerging evidence has manifested that circRNAs affect the stability or translation of target mRNAs by sponging miRNAs, thereby modulating gene expression at the transcriptional level (Cui et al., 2018; Zhong et al., 2018). Also, circRNAs occupy a crucial position in

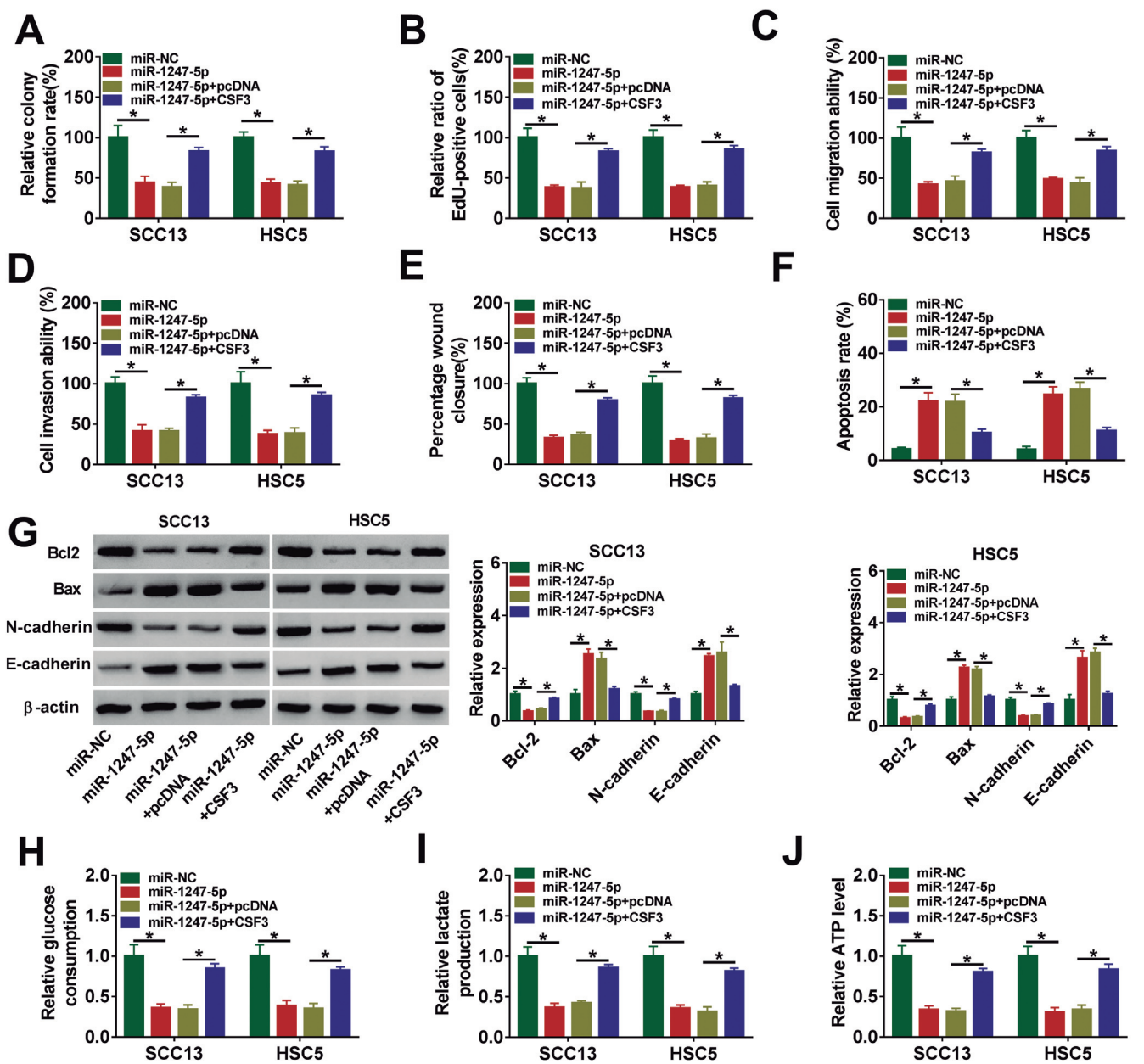

Fig. 6. CSF3 restored the inhibitory effect of miR-1247-5p on CSCC cell progression. SCC13 and HSC5 cells were introduced with miR-NC, miR-1247-5p, miR-1247-5p+pcDNA or miR-1247-5p+CSF3. **A, B.** Cell proliferation was tested using colony formation assay and EdU assay. **C-E.** Transwell and wound healing assays were applied to detect cell migration and invasion. **F.** Cell apoptosis was assessed by flow cytometry. **G.** The levels of apoptosis-related and invasion-related proteins were examined by Western blot. **H-J.** Glucose consumption, lactate production, and ATP level were examined using corresponding commercial kits. *P<0.05.

biological processes by functioning as ceRNAs. In the current research, miRNAs that might bind to circEBF1 were predicted using bioinformatics tools. According to experimental verification, we evidenced that circEBF1 sponged miR-1247-5p.

Several previous studies revealed that miR-1247-5p functioned as a pivotal regulator in the prognosis and progression of many cancers. For instance, Chu et al. found that miR-1247-5p restoration alleviated the malignant behavior of hepatocellular carcinoma through inhibition of Wnt3 (Chu et al., 2017). Zeng et al. suggested that the down-regulation of miR-1247-5p was tightly related to poor prognosis of breast cancer, and miR-1247-5p up-regulation suppressed breast cancer progression by repressing DVL1 (Zeng et al., 2018). Additionally, miR-1247-5p undermined the promotion of circ_0070934 on CSCC progression (An et al., 2019). Herein, we validated that miR-1247-5p level was strikingly reduced in CSCC, and miR-1247-5p augmentation counteracted the inhibition of circEBF1 interference on CSCC progression.

Accumulating evidence has identified that miRNAs can induce mRNA degradation or block its translation by base-pairing with mRNA 3'UTR (Thomas et al., 2010). Our research confirmed that miR-1247-5p directly targeted CSF3 according to bioinformatics analysis and experimental verification. CSF3 (also known as G-CSF) is a cytokine that can regulate the proliferation and

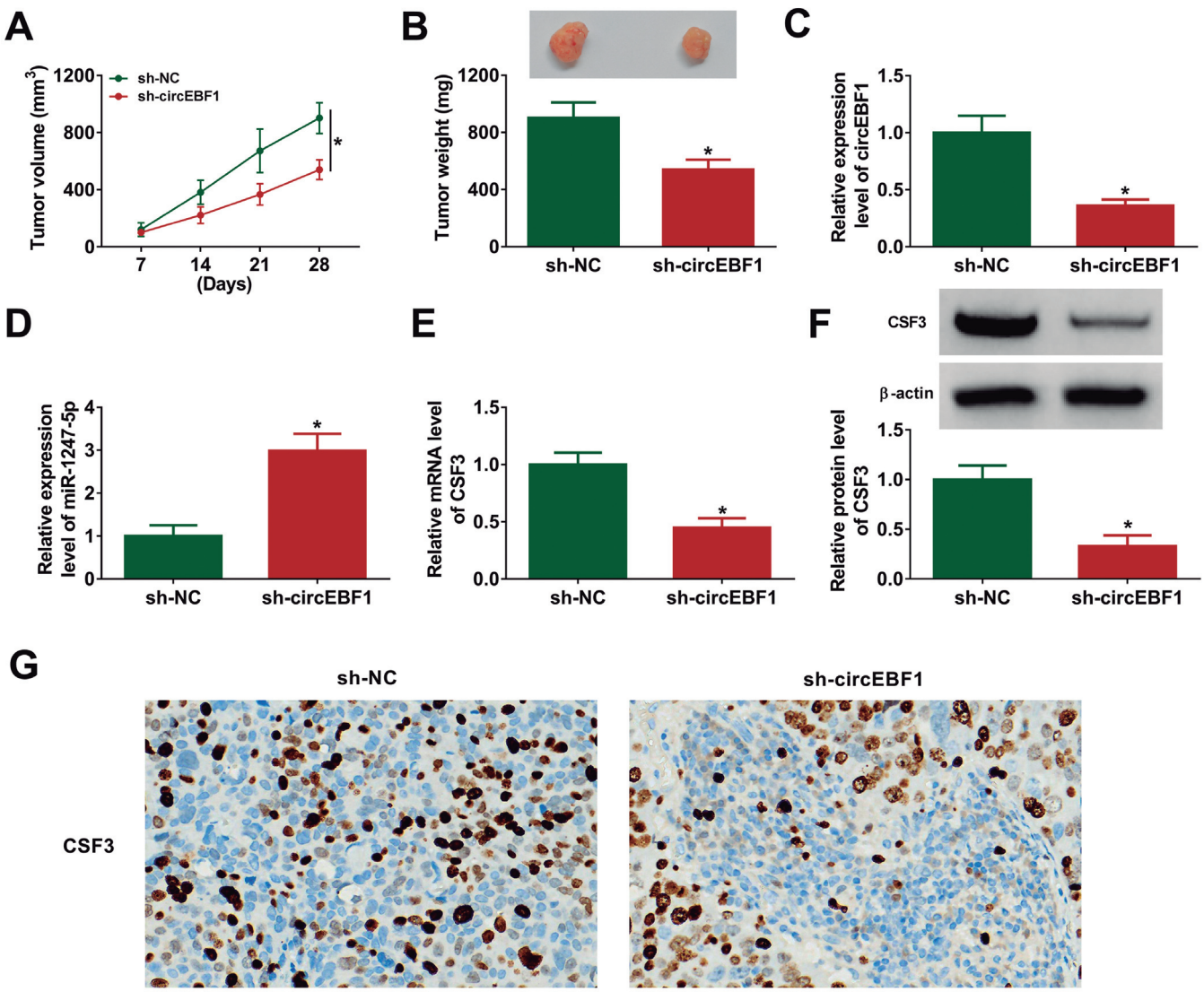

Fig. 7. Silencing of circEBF1 hindered CSCC growth *in vivo*. HSC5 cells stably expressing sh-NC or sh-circEBF1 were injected into nude mice. **A.** The expression of circEBF1 was detected using qRT-PCR. **B.** Tumor volume was measured every 7 days. **C.** After the mice were sacrificed, the tumors were photographed and weighed. **D-F.** The levels of miR-1247-5p and CSF3 were examined by qRT-PCR or Western blot. **G.** CSF3 expression was determined by IHC analysis in tumor tissues. *P<0.05. G, x 100.

differentiation of mature granulocytes (Bendall and Bradstock, 2014). Recent reports have disclosed that G-CSF contributes to tumor metastasis by mediating tumor-related neutrophils (Yeo et al., 2018). In neuroblastoma, G-CSF facilitated tumor growth and metastasis by activating STAT3 (Agarwal et al., 2015). Additionally, Karagiannidis et al. found that G-CSF expedited colon tumor growth by regulating T cell response (Karagiannidis et al., 2020). A recent study indicated that CSF3 level was remarkably increased in CSCC (Das Mahapatra et al., 2020), which was in agreement with our results. Furthermore, we demonstrated that miR-1247-5p restrained CSCC cell progression by binding to CSF3. Mechanistically, circEBF1 up-regulated CSF3 expression by sponging miR-1247-5p.

In conclusion, this research revealed that circEBF1 facilitated CSCC progression by absorbing miR-1247-5p and up-regulating CSF3 expression. Furthermore, the discovery of new ceRNA mechanisms might provide promising biomarkers and therapeutic targets for CSCC.

Acknowledgements. None.

Disclosure of interest. The authors declare that they have no financial conflicts of interest.

Funding. None.

Ethics approval. All procedures were approved by the Institutional Animal Care and Use Committee of Shanxi Provincial People's Hospital.

References

Agarwal S., Lakoma A., Chen Z., Hicks J., Metelitsa L.S., Kim E.S. and Shohet J.M. (2015). G-CSF promotes neuroblastoma tumorigenicity and metastasis via STAT3-dependent cancer stem cell activation. Cancer Res. 75, 2566-2579.

An X., Liu X., Ma G. and Li C. (2019). Upregulated circular RNA circ_0070934 facilitates cutaneous squamous cell carcinoma cell growth and invasion by sponging miR-1238 and miR-1247-5p. Biochem. Biophys. Res. Commun. 513, 380-385.

Bendall L.J. and Bradstock K.F. (2014). G-csf: From granulopoietic stimulant to bone marrow stem cell mobilizing agent. Cytokine Growth Factor Rev. 25, 355-367.

Braicu C., Zimta A.A., Gulei D., Olariu A. and Berindan-Neagoe I. (2019). Comprehensive analysis of circular RNAs in pathological states: Biogenesis, cellular regulation, and therapeutic relevance. Cell Mol. Life Sci. 76, 1559-1577.

Chen L., Yang X., Zhao J., Xiong M., Almaraihah R., Chen Z. and Hou T. (2020a). Circ_0008532 promotes bladder cancer progression by regulation of the miR-155-5p/miR-330-5p/MTGR1 axis. J. Exp. Clin. Cancer Res. 39, 94.

Chen S., Ding J., Wang Y., Lu T., Wang L., Gao X., Chen H., Qu L. and He C. (2020b). RNA-seq profiling of circular RNAs and the oncogenic role of CIRCPVT1 in cutaneous squamous cell carcinoma. Onco Targets Ther. 13, 6777-6788.

Chu Y., Fan W., Guo W., Zhang Y., Wang L., Guo L., Duan X., Wei J. and Xu G. (2017). MiR-1247-5p functions as a tumor suppressor in human hepatocellular carcinoma by targeting Wnt3. Oncol. Rep. 38, 343-351.

Cui X., Wang J., Guo Z., Li M., Li M., Liu S., Liu H., Li W., Yin X., Tao J. and Xu W. (2018). Emerging function and potential diagnostic value of circular RNAs in cancer. Mol. Cancer 17, 123.

Das Mahapatra K., Pasquali L., Sondergaard J.N., Lapins J., Nemeth I.B., Baltas E., Kemeny L., Homey B., Moldovan L.I., Kjems J., Kutter C., Sonkoly E., Kristensen L.S. and Pivarcsi A. (2020). A comprehensive analysis of coding and non-coding transcriptomic changes in cutaneous squamous cell carcinoma. Sci. Rep. 10, 3637.

Gao L., Jin H.J., Zhang D. and Lin Q. (2020). Silencing circRNA_001937 may inhibit cutaneous squamous cell carcinoma proliferation and induce apoptosis by preventing the sponging of the miRNA5973p/FOSL2 pathway. Int. J. Mol. Med. 46, 1653-1660.

Garcia-Sancha N., Corchado-Cobos R., Perez-Losada J. and Canueto J. (2019). MicroRNA dysregulation in cutaneous squamous cell carcinoma. Int. J. Mol. Sci. 20.

Harper K.L., McDonnell E. and Whitehouse A. (2019). CircRNAs: From anonymity to novel regulators of gene expression in cancer (review). Int. J. Oncol. 55, 1183-1193.

Inman G.J., Wang J., Nagano A., Alexandrov L.B., Purdie K.J., Taylor R.G., Sherwood V., Thomson J., Hogan S., Spender L.C., South A.P., Stratton M., Chelala C., Harwood C.A., Proby C.M. and Leigh I.M. (2018). The genomic landscape of cutaneous SCC reveals drivers and a novel azathioprine associated mutational signature. Nat. Commun. 9, 3667.

Karagiannidis I., Jerman S.J., Jacenik D., Phinney B.B., Yao R., Prossnitz E.R. and Beswick E.J. (2020). G-CSF and G-CSFR modulate CD4 and CD8 T cell responses to promote colon tumor growth and are potential therapeutic targets. Front. Immunol. 11, 1885.

Karia P.S., Han J. and Schmults C.D. (2013). Cutaneous squamous cell carcinoma: Estimated incidence of disease, nodal metastasis, and deaths from disease in the united states, 2012. J. Am. Acad. Dermatol. 68, 957-966.

Konicke K., Lopez-Luna A., Munoz-Carrillo J.L., Servin-Gonzalez L.S., Flores-de la Torre A., Olasz E. and Lazarova Z. (2018). The microRNA landscape of cutaneous squamous cell carcinoma. Drug Discov. Today 23, 864-870.

Li J., Sun D., Pu W., Wang J. and Peng Y. (2020). Circular RNAs in cancer: Biogenesis, function, and clinical significance. Trends Cancer 6, 319-336.

Li X., Zhou C., Zhang C., Xie X., Zhou Z., Zhou M., Chen L. and Ding Z. (2019). MicroRNA-664 functions as an oncogene in cutaneous squamous cell carcinomas (CSCC) via suppressing interferon regulatory factor 2. J. Dermatol. Sci. 94, 330-338.

Nagarajan P., Asgari M.M., Green A.C., Guhan S.M., Arron S.T., Proby C.M., Rollison D.E., Harwood C.A. and Toland A.E. (2019). Keratinocyte carcinomas: Current concepts and future research priorities. Clin. Cancer Res. 25, 2379-2391.

Navarrete-Dechent C., Veness M.J., Droppelmann N. and Uribe P. (2015). High-risk cutaneous squamous cell carcinoma and the emerging role of sentinel lymph node biopsy: A literature review. J. Am. Acad. Dermatol. 73, 127-137.

Que S.K.T., Zwald F.O. and Schmults C.D. (2018). Cutaneous squamous cell carcinoma: Management of advanced and high-stage tumors. J. Am. Acad. Dermatol. 78, 249-261.

Ratushny V., Gober M.D., Hick R., Ridky T.W. and Seykora J.T. (2012). From keratinocyte to cancer: The pathogenesis and modeling of cutaneous squamous cell carcinoma. J. Clin. Invest. 122, 464-472.

Sand M., Bechara F.G., Gambichler T., Sand D., Bromba M., Hahn S.A., Stockfleth E. and Hessam S. (2016). Circular RNA expression in cutaneous squamous cell carcinoma. J. Dermatol. Sci. 83, 210-218.

Slack F.J. and Chinnaiyan A.M. (2019). The role of non-coding RNAs in oncology. Cell 179, 1033-1055.

Thomas M., Lieberman J. and Lal A. (2010). Desperately seeking microRNA targets. Nat. Struct. Mol. Biol. 17, 1169-1174.

Wang Y., Yin L. and Sun X. (2020). CircRNA hsa_circ_0002577 accelerates endometrial cancer progression through activating IGF1R/PI3K/AKT pathway. J. Exp. Clin. Cancer Res. 39, 169.

Yeo B., Redfern A.D., Mouchemore K.A., Hamilton J.A. and Anderson R.L. (2018). The dark side of granulocyte-colony stimulating factor: A supportive therapy with potential to promote tumour progression. Clin. Exp. Metastasis 35, 255-267.

Yesantharao P., Wang W., Ioannidis N.M., Demehri S., Whittemore A.S. and Asgari M.M. (2017). Cutaneous squamous cell cancer (CSCC) risk and the human leukocyte antigen (HLA) system. Hum. Immunol. 78, 327-335.

Yu X. and Li Z. (2016). The role of miRNAs in cutaneous squamous cell carcinoma. J. Cell Mol. Med. 20, 3-9.

Zeng B., Li Y., Feng Y., Lu M., Yuan H., Yi Z., Wu Y., Xiang T., Li H. and Ren G. (2018). Downregulated miR-1247-5p associates with poor prognosis and facilitates tumor cell growth via DVL1/Wnt/beta-catenin signaling in breast cancer. Biochem. Biophys. Res. Commun. 505, 302-308.

Zhang D.W., Wu H.Y., Zhu C.R. and Wu D.D. (2020). CircRNA hsa_circ_0070934 functions as a competitive endogenous RNA to regulate HOXb7 expression by sponging miR12363p in cutaneous squamous cell carcinoma. Int. J. Oncol. 57, 478-487.

Zhang H.D., Jiang L.H., Sun D.W., Hou J.C. and Ji Z.L. (2018). CircRNA: A novel type of biomarker for cancer. Breast Cancer 25, 1-7.

Zhong Y., Du Y., Yang X., Mo Y., Fan C., Xiong F., Ren D., Ye X., Li C., Wang Y., Wei F., Guo C., Wu X., Li X., Li Y., Li G., Zeng Z. and Xiong W. (2018). Circular RNAs function as ceRNAs to regulate and control human cancer progression. Mol. Cancer 17, 79.

Accepted May 11, 2022